



HAL
open science

Geometry of dislocations in icosahedral quasicrystals

Denis Gratias, Jean-Tristan Beauchesne, Frédéric Mompiou, Daniel Caillard

► **To cite this version:**

Denis Gratias, Jean-Tristan Beauchesne, Frédéric Mompiou, Daniel Caillard. Geometry of dislocations in icosahedral quasicrystals. *Philosophical Magazine*, 2006, 86 (25-26), pp.4139-4151. 10.1080/14786430600575435 . hal-00513660

HAL Id: hal-00513660

<https://hal.science/hal-00513660>

Submitted on 1 Sep 2010

HAL is a multi-disciplinary open access archive for the deposit and dissemination of scientific research documents, whether they are published or not. The documents may come from teaching and research institutions in France or abroad, or from public or private research centers.

L'archive ouverte pluridisciplinaire **HAL**, est destinée au dépôt et à la diffusion de documents scientifiques de niveau recherche, publiés ou non, émanant des établissements d'enseignement et de recherche français ou étrangers, des laboratoires publics ou privés.

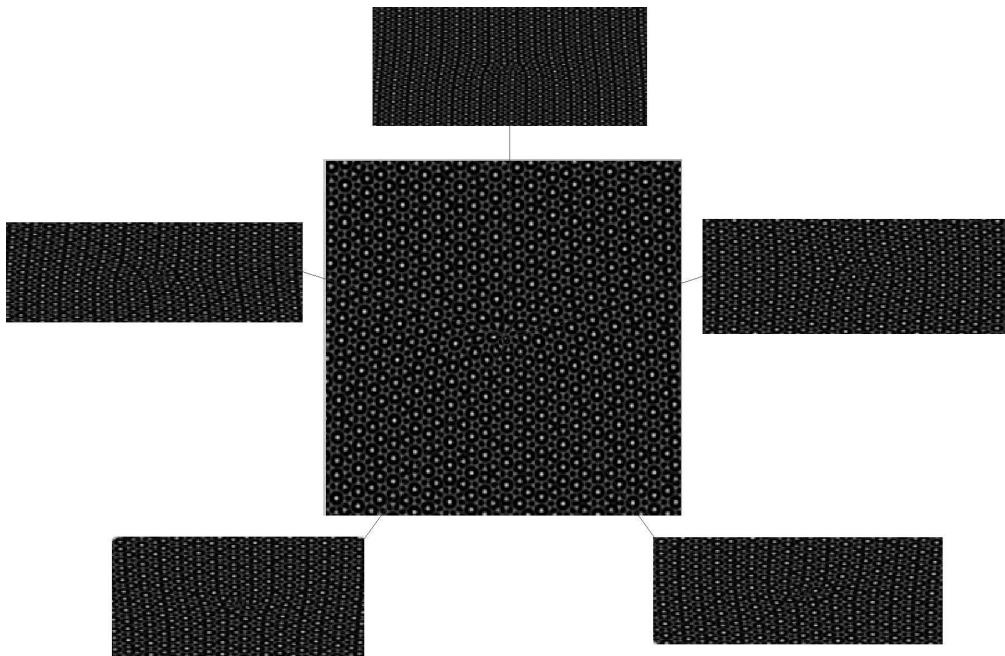


Geometry of dislocations in icosahedral quasicrystals

Journal:	<i>Philosophical Magazine & Philosophical Magazine Letters</i>
Manuscript ID:	TPHM-05-Oct-0459.R1
Journal Selection:	Philosophical Magazine
Date Submitted by the Author:	06-Jan-2006
Complete List of Authors:	Gratias, Denis; CNRS-ONERA, LEM Beauchesne, Jean-Tristan; ONERA, LEM Momprou, Frederic; NIST, Metallurgy Caillard, Daniel; CEMES - CNRS, Laboratoire d'Optique Electronique
Keywords:	quasicrystalline alloys, dislocation theory
Keywords (user supplied):	quasicrystal, dislocation, plasticity
<p>Note: The following files were submitted by the author for peer review, but cannot be converted to PDF. You must view these files (e.g. movies) online.</p> <p>DGratiasetal.tex</p>	

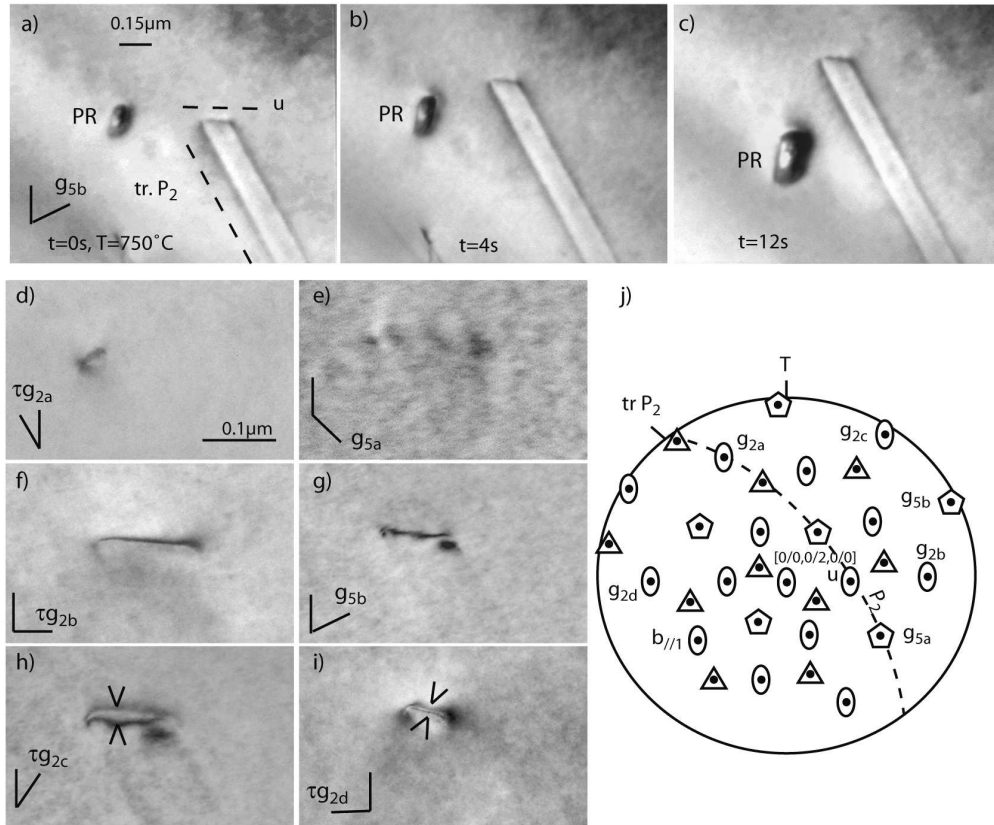


1
2
3
4
5
6
7
8
9
10
11
12
13
14
15
16
17
18
19
20
21
22
23
24
25
26
27
28
29
30
31
32
33
34
35
36
37
38
39
40
41
42
43
44
45
46
47
48
49
50
51
52
53
54
55
56
57
58
59
60



152x99mm (300 x 300 DPI)

Review Only

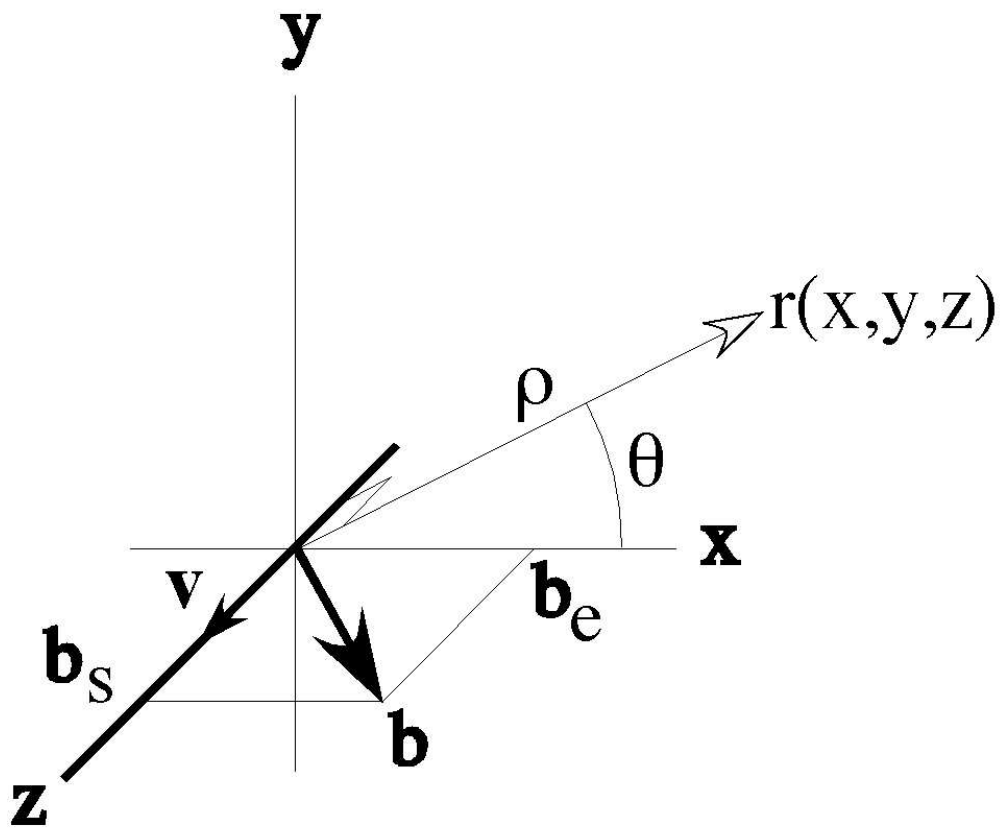


141x116mm (300 x 300 DPI)

Manuscript Only

1
2
3
4
5
6
7
8
9
10
11
12
13
14
15
16
17
18
19
20
21
22
23
24
25
26
27
28
29
30
31
32
33
34
35
36
37
38
39
40
41
42
43
44
45
46
47
48
49
50
51
52
53
54
55
56
57
58
59
60

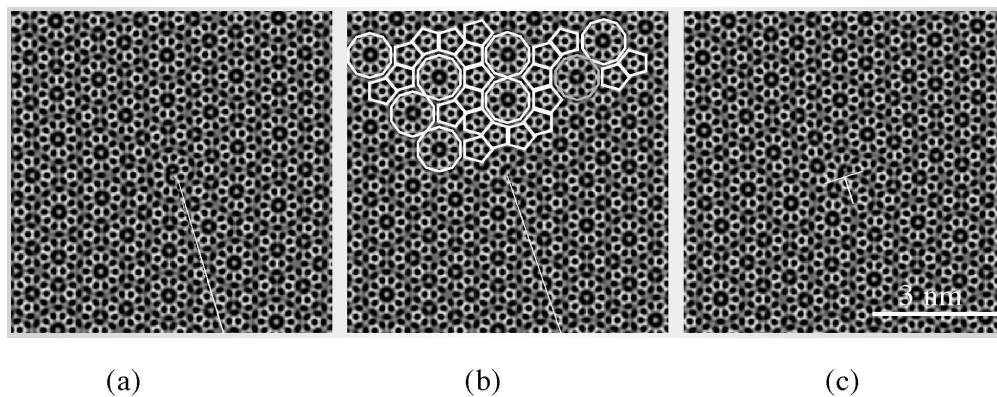
1
2
3
4
5
6
7
8
9
10
11
12
13
14
15
16
17
18
19
20
21
22
23
24
25
26
27
28
29
30
31
32
33
34
35
36
37
38
39
40
41
42
43
44
45
46
47
48
49
50
51
52
53
54
55
56
57
58
59
60



81x69mm (300 x 300 DPI)

Only

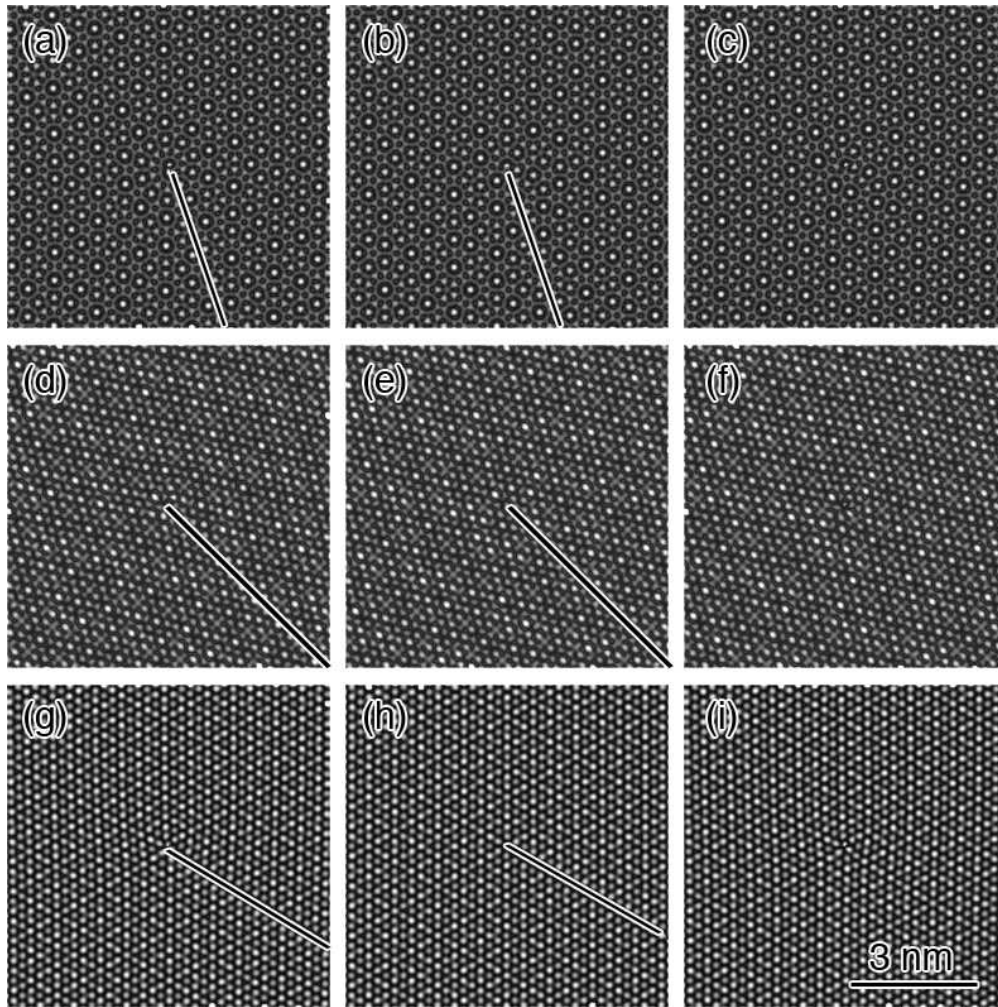
1
2
3
4
5
6
7
8
9
10
11
12
13
14
15
16
17
18
19
20
21
22
23
24
25
26
27
28
29
30
31
32
33
34
35
36
37
38
39
40
41
42
43
44
45
46
47
48
49
50
51
52
53
54
55
56
57
58
59
60



165x64mm (300 x 300 DPI)

Peer Review Only

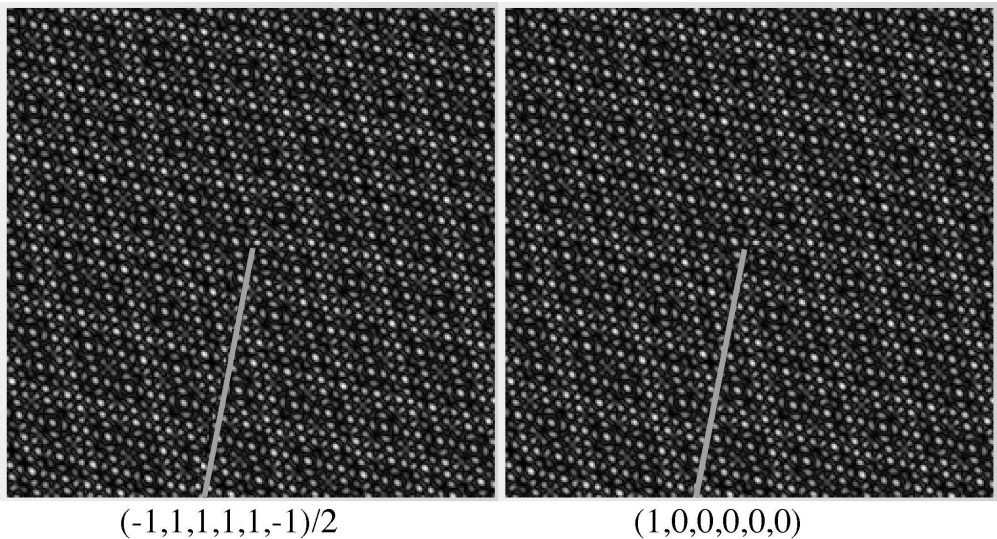
1
2
3
4
5
6
7
8
9
10
11
12
13
14
15
16
17
18
19
20
21
22
23
24
25
26
27
28
29
30
31
32
33
34
35
36
37
38
39
40
41
42
43
44
45
46
47
48
49
50
51
52
53
54
55
56
57
58
59
60



279x280mm (72 x 72 DPI)



1
2
3
4
5
6
7
8
9
10
11
12
13
14
15
16
17
18
19
20
21
22
23
24
25
26
27
28
29
30
31
32
33
34
35
36
37
38
39
40
41
42
43
44
45
46
47
48
49
50
51
52
53
54
55
56
57
58
59
60



184x99mm (300 x 300 DPI)

Review Only

Geometry of dislocations in icosahedral quasicrystals

Denis Gratias, Jean-Tristan Beauchesne,
LEM-CNRS/ONERA, B.P. 72
92322 Châtillon cedex, France

Frédéric Momprou,
Metallurgy Division, NIST,
100 Bureau Dr. stop 8555
Gaithersburg 20899 MD, USA

and Daniel Caillard
CEMES-CNRS,
29, rue Jeanne Marvig B.P. 4347
31055 Toulouse cedex 4, France

Abstract

Quasicrystals are complex metallic alloys that are ductile at high temperatures close to their melting point. It has been early recognized that their plasticity is due to a flux of moving linear defects in all respects similar to dislocations in ordinary crystals. The present paper is an attempt to propose in a short didactic review a simple synthetic analysis of the basic underlying geometry of quasicrystalline dislocations exemplified with experimental and calculated images of electron microscopy in icosahedral phases.

1 Introduction

This paper is a short contribution to the analysis of the geometrical properties of dislocations in icosahedral quasicrystals [1, 2]. Its main goal is to present, as a short review, a detailed description of these defects in the framework of N -dimensional crystallography.

It has been early recognized that, like many other intermetallic compounds, icosahedral quasicrystals are very brittle at low temperature but exhibit a unusually large plastic regime at high temperatures

which is essentially due to the motion of linear defects in all respects similar to ordinary dislocations (see for instance [3, 4]).

From a geometrical point of view, these original deformation modes are qualified as dislocations [5, 6, 7, 8] because by its very definition, a (icosahedral) quasicrystal can be described as the $3D$ cut along an irrational orientation of an abstract $6D$ -periodic object [9, 10, 11, 12]. As periodicity is recovered in this abstract $6D$ space, the notion of dislocation is a natural extension of the one classically defined for crystals. This abstract $6D$ space decomposes into two complementary subspaces :

- the $3D$ physical space that we shall call the parallel space and note E_{\parallel} ;
- the perpendicular space, also of dimension 3, that we note E_{\perp} .

Quasiperiodic structures present in real space atomic planes and rows, exactly like ordinary crystals with the only difference that the constitutive atoms are not periodically but quasiperiodically spaced (see for instance [9]). An important theorem [13] states that for the case where the $6D$ lattice nodes project onto E_{\perp} as an uniformly dense set of points — as it is the case of the icosahedral phase — *any two parallel cuts along E_{\parallel} generate locally isomorphic quasicrystalline structures that are physically equivalent to any finite distance, i. e.* any two such quasicrystals are *physically indistinguishable* in all respects. This basic gauge invariance corresponds to the fact that the physical properties of quasicrystalline dislocations must be independent of the choice of origin in E_{\perp} during the cut process generating the real atomic structure. As we shall see next, this invariance induces important geometric constraints in the description of quasicrystalline dislocations.

2 Geometry of quasicrystalline dislocations

2.1 Burgers vector

The definition of a dislocation in a (Euclidean) N -dimensional (ND) medium follows the Volterra process used for usual $3D$ media : a cut is performed along a $(N - 1)D$ oriented (hyper)surface Σ bounded by a closed $(N - 2)D$ (hyper) line; the *upper* part of the medium at the cut level is displaced by a finite vector \vec{B} , with respect to the *lower* part. The medium is finally re-glued and mechanically relaxed.

1
2
3
4
5
6
7
8
9
10
11
12
13
14
15
16
17
18
19
20
21
22
23
24
25
26
27
28
29
30
31
32
33
34
35
36
37
38
39
40
41
42
43
44
45
46
47
48
49
50
51
52
53
54
55
56
57
58
59
60

If \vec{B} is a translation belonging to the translation invariance group of the medium, the Σ cut surface vanishes and an elastic singularity is created at the level of the (hyper)line that we call a *perfect dislocation* with Burgers vector \vec{B} . For the case of a ND -periodic object with hyperlattice Λ , the Burgers vector \vec{B} of a perfect dislocation is a hyperlattice translation : $\vec{B} \in \Lambda$ and therefore *it has necessarily one non zero components in each E_{\parallel} and E_{\perp} subspaces:*

$$\vec{B} = \vec{b}_{\parallel} + \vec{b}_{\perp} \in \Lambda \quad (1)$$

An example of a (computed) dislocation, seen end on, of Burgers vector $B = (0, 0, 1, 0, 0, -1)$ ($6D$ notation from the indexing scheme proposed by Cahn et al. [14]) in an icosahedral phase is presented on Fig. 1. The observation plane is perpendicular to a 5-fold direction. As for ordinary dislocations, observation at glancing angle along certain directions shows kinds of additional half-planes the number and stacking of which depends on the chosen direction.

2.2 Dislocation line

The dislocation line, noted V , is a $(N - 2)D$ -manifold. For the icosahedral case, the line V is a $6 - 2 = 4D$ manifold. Closed circuits can be constructed around V in the remaining $2D$ -subspace, that will be used to define the Burgers vector. This means that Burgers circuits are entirely defined in E_{\parallel} and are indeed pertinent physical quantities that can be experimentally determined¹.

The invariance stating that the dislocation description is independent of the choice of the origin in E_{\perp} fixes the "orientation" of the dislocation line V : the only generic way for V to be invariant by any translation of the cut along E_{\perp} , is that V contains E_{\perp} . The dislocation $4D$ -line decomposes therefore into a $3D$ -subspace parallel to E_{\perp} plus a remaining $1D$ -subspace that is necessarily in E_{\parallel} : this is the usual real dislocation line \vec{u} in physical space.

Thus a (perfect) dislocation in an icosahedral quasicrystal is made of a Burgers vector \vec{B} belonging to the $6D$ -lattice of the quasicrystal and a dislocation line of dimension 4 that decomposes into a $1D$ line in E_{\parallel} and a $3D$ -subspace parallel to E_{\perp} . It formally decomposes as $V = \vec{v}_{\parallel} \oplus E_{\perp}$.

Since \vec{B} has a non zero component in E_{\perp} it is *stricto sensu*, impossible to construct pure edge (perfect) dislocations in an icosahedral

¹This does not imply \vec{B} to lie in this $2D$ -subspace: in fact \vec{B} is in a rational $2D$ -plane with respect to Λ that is oblique with respect to E_{\parallel} . It is the irrationality of this oblique orientation that makes the relation between the lattice nodes of this rational plane and their projections in E_{\parallel} a one-to-one correspondence.

1
2
3
4
5
6
7
8
9
10
11
12
13
14
15
16
17
18
19
20
21
22
23
24
25
26
27
28
29
30
31
32
33
34
35
36
37
38
39
40
41
42
43
44
45
46
47
48
49
50
51
52
53
54
55
56
57
58
59
60

phase because of E_{\perp} being embedded in V . Hence, *edge* and *screw* dislocations are better defined in quasicrystals in *considering only the relative orientation of the Burgers vector with respect to the real physical space irrespective of the components of the Burgers vector onto E_{\perp}* . We thus define the edge and screw components, respectively \vec{b}_e and \vec{b}_s of a dislocation by the usual scalar products $\vec{b}_s = (\vec{b}_{\parallel} \cdot \vec{u}_{\parallel})\vec{u}_{\parallel}$, and $\vec{b}_e = \vec{b}_{\parallel} - \vec{b}_s$.

If the dislocation line \vec{u}_{\parallel} has a specific orientation along well defined quasicrystallographic directions (as it is often the case in crystals), the corresponding $4D$ dislocation (straight) line V contains a $2D$ -sublattice of Λ the trace of which in E_{\parallel} is the physical dislocation line \vec{u}_{\parallel} .

2.3 Displacement field induced by a quasicrystalline dislocation

As imposed by the decomposition (1) any dislocation in a quasicrystal generates two displacement fields of different physical nature.

The first one is related to the parallel component \vec{b}_{\parallel} of the $6D$ Burgers vector \vec{B} and is governed, in a good approximation, by standard elastic theory. Its stored elastic energy varies like $|b_{\parallel}|^2$ and the interaction forces between dislocations and stress fields can be computed using the usual tools of elasticity theory. This displacement field is referred to as the *phonon* field although — irrespective of a global dislocation motion — it describes static displacements of atoms.

The second displacement field is non trivial and is specific to quasicrystals and incommensurate structures. It is generated by the perpendicular component \vec{b}_{\perp} of the $6D$ Burger vector and extends in E_{\perp} . It is not attached to any local elastic displacement of atoms but to a *rearrangement of the local atomic configurations with respect to each others with no change in their shapes*. It is closely related to the configurational energy of the alloy on both chemical and topological order and is depend on the thermodynamic aspects of the material. It is (improperly) called the *phason* field as a reference to the phason modes encountered in dynamical studies of incommensurate structures. The expression of the energy attached to this phason field is either proportional to $|b_{\perp}|$ or $|b_{\perp}|^2$ depending on which model (perfect tiling or random tiling) is chosen to explain the stability of the quasicrystal. So far, the most advanced study on the subject has been made on decagonal phases by Koschella [20] who concluded that the phason energy is best described by a quadratic term in phason fluctuations. In that scheme, the dislocation energy associated to the local tiling faults around the dislocation would vary as $|b_{\perp}|^2$.

The global $6D$ -displacement field \vec{U} induced by a dislocation decomposes on respectively E_{\parallel} and E_{\perp} as $\vec{U} = \vec{u}_{\parallel} + \vec{u}_{\perp}$. The displacement field $\vec{U}(\vec{X})$ depends only on the parallel component, x_{\parallel} , of the running vector \vec{X} , so that:

$$\vec{U}(\vec{X}) = \vec{U}(x_{\parallel}) = \vec{u}_{\parallel}(x_{\parallel}) + \vec{u}_{\perp}(x_{\parallel})$$

as the dislocation "line" contains E_{\perp} so that the total $6D$ -displacement field depends only on the physical space variable. Integrated along a closed circuit C_{\parallel} in E_{\parallel} , these two fields lead to:

$$\oint_{C_{\parallel}} d\vec{u}_{\parallel} = \vec{b}_{\parallel} \quad \oint_{C_{\parallel}} d\vec{u}_{\perp} = \vec{b}_{\perp}$$

if the circuit encloses the dislocation line V , and zero otherwise.

2.4 Partial dislocations and dissociations

The notion of partial dislocations in quasicrystals follows the one defined for crystals: a partial dislocation has a Burger vector that is an integer fraction of a lattice translation. Such dislocations are bounded by $2D$ extended faults with fault vectors equal to the Burgers vector (up to a lattice translation of Λ). The i -AlPdMn F-type icosahedral phase has specific atomic structures where the atoms distribute on three main quasiperiodic networks displaced from each other by $(1, 0, 0, 0, 0, 0)$ and $(\bar{1}, 1, 1, 1, 1, \bar{1})/2$. These translations and their combinations can be called *super partial* dislocations in the sense that they belong to the $P(A)$ -lattice for $(1, 0, 0, 0, 0, 0)$ and $D_{x(y)}^6(A)$ -lattice for $(\bar{1}, 1, 1, 1, 1, \bar{1})/2$ which both are superlattices of rank 2 of the $F(2A)$ -lattice. These translations are good candidates for possibly generating antiphase boundaries (both with phase shifts 0 or π in the $6D$ space) in the material. So far only superpartial dislocations of Burgers vectors $(1, 0, 0, 0, 0, 0)$ and $(1, 0, \bar{1}, 0, 0, 1)$, both of the same family, have been observed in these phases [24].

Quasicrystals exhibit a specific type of dissociation that results from the very basic physical dissymmetry between the phonon and the phason spaces in the canonical decomposition $\vec{B} = \vec{b}_{\parallel} + \vec{b}_{\perp}$. A dislocation appears as a strip of fault bounded on the head, by the singularity \vec{b}_{\parallel} , and on the tail, by \vec{b}_{\perp} . All the elastic distortion is concentrated on the head line whereas the tail line corresponds to the termination of the phason wall of the strip and carries no distortions but only tile mismatches. The motion of the dislocation is therefore governed by two mechanisms: the first one, on the head, is driven by the usual elastic interactions with stress fields, whereas the second

one, related to phasons, depends on the chemical ordering driving forces of the structure. The former mechanism induces possible fast motions but the latter one, relying on atomic diffusion, can have a much longer relaxation time depending on temperature. This suggests a scenario of dislocations being immobile at low temperature, having a slow motion and trailing a more or less extended phason wall at intermediate temperatures and eventually an easy viscous motion at higher temperatures as will be discussed next.

2.5 Glide and climb in quasicrystals

Formally the glide manifold associated to a dislocation is defined by the union of the dislocation line V and the Burgers vector \vec{B} . As in ordinary crystals, a motion of the dislocation line in the glide manifold is conservative in the sense that it generates no long distance mass transport. In the icosahedral case, it is a generic $5D$ -space that decomposes into a $3D$ -space parallel to E_{\perp} plus a $2D$ -manifold in E_{\parallel} that is the actual glide plane if the dislocation line is a straight line. If this straight line is along a quasicrystalline direction, then the generic glide $5D$ -manifold contains a $3D$ -sublattice of Λ defined by the $2D$ -sublattice of Λ contained in V and the Burgers vector \vec{B} itself. The remaining $2D$ -subspace is spanned by two directions that are irrationally oriented with respect to Λ and embedded in E_{\perp} .

Climb is defined as a motion direction of the dislocation line that has a non zero component outside the glide manifold. For example, this is the case for a dislocation moving along the direction $\vec{b}_{\parallel} \wedge \vec{v}_{\parallel}$ in E_{\parallel} which corresponds to pure climb motion like in ordinary crystals. It is a non-conservative motion that requires atomic propagation to long distance.

Because the motion of a perfect dislocation requires a re-tiling around the dislocation line, we can analyze it as a two-step process: a (pure phonon) motion characterized by \vec{b}_{\parallel} followed by the chemical reordering (pure phason) and re-tiling characterized by \vec{b}_{\perp} .

The question arises of what direction of motion, say \vec{d}_{\parallel} , would be optimum for the sole phonon field propagation irrespective of the phason field reconstruction.

We first notice atoms in quasicrystals distribute along (quasicrystalline) rows and planes as in crystals. Therefore, we may expect quasilattice friction to play a role with the existence of quasiperiodically spaced Peierls valleys along which dislocation lines would be preferentially oriented. For the same reasons, we assume that the direction of motion to be a quasicrystallographic direction, *i.e.* \vec{d}_{\parallel} can be considered, irrespective of a length factor, as the projection of a

6D node of Λ which, in turn, has a single image \vec{d}_\perp in E_\perp . We assume the dislocation line \vec{v}_\parallel to also be a straight line aligned along another quasicrystallographic direction not collinear to \vec{d}_\parallel where, as previously, \vec{v}_\parallel is the projection of a 6D-lattice node with image \vec{v}_\perp in E_\perp .

The surface swept by the dislocation during the motion is a 5D-space generated by the dislocation line V (a 4D-manifold) plus the direction of motion \vec{d}_\parallel . This 5D-space, say S , contains a 4D-sublattice of Λ embedded in the 4D-subspace, say Σ , generated by $(\vec{v}_\parallel, \vec{v}_\perp, \vec{d}_\parallel, \vec{d}_\perp)$. The remaining dimension corresponds to a direction Δ that is necessarily in E_\perp — since Σ contains a 2D-plane only $(\vec{v}_\perp, \vec{d}_\perp)$ of the 3D-space E_\perp — and therefore irrationally oriented with respect to Λ . For the displacement by \vec{b}_\parallel of the matter during the dislocation motion to respect the tiling matching with no overlaps and empty spaces, the 4D-sublattice embedded in S , that represents the part of the tiling vertices that form the matches on the Σ surface, must be kept invariant up to the global translation \vec{b}_\parallel in E_\parallel .

This is achieved if \vec{b}_\perp has a zero component in Σ and thus is aligned along Δ . This induces $\vec{b}_\perp \perp \vec{d}_\perp$ and $\vec{b}_\perp \perp \vec{v}_\perp$. Because for any two vectors \vec{A} and \vec{B} of Λ , a zero scalar product of their projections in either the spaces E_\parallel or E_\perp implies the same zero value for the scalar product of the projections in the other space:

$$\vec{A}, \vec{B} \in \Lambda, \quad \vec{a}_\parallel \cdot \vec{b}_\parallel = 0 \leftrightarrow \vec{a}_\perp \cdot \vec{b}_\perp = 0$$

so that $\vec{b}_\parallel \perp \vec{d}_\parallel$ and $\vec{b}_\parallel \perp \vec{v}_\parallel$. Hence, we can conclude that the dislocation motion that keeps the internal tiling coherent — with no empty spaces or overlaps in the trace of motion — is obtained for *pure edge* dislocation ($\vec{b}_\parallel \perp \vec{v}_\parallel$) moving in a *pure climb* fashion ($\vec{b}_\parallel \perp \vec{d}_\parallel$).

This problem of glide versus climb in the dislocation motion in *i*-AlPdMn has been the object of interesting debates in these last years. Most of the early heuristic models of dislocation motion in *i*-AlPdMn where primarily focused on glide mechanisms [18, 19]. Due to the large dependence of mechanical properties on temperature, they aimed at describing macroscopic parameters in the framework of thermally activated dislocation motion. The thermally activated events were assumed to correspond to the overcoming of atomic clusters or of a quasi-periodic Peierls barrier. They accounted for activation parameters satisfactorily at low temperatures and high stresses. However, since the year 2000, numerous experimental evidences for climb have been found in as cast *i*-AlPdMn [21, 22, 23], deformed at low [24] and at high temperatures [25]. Nowadays, although it seems that climb has been accepted as the major mechanism of plastic deformation of *i*-AlPdMn at high temperature.

Figure 2 shows a dislocation d moving at 750 °C in i -AlPdMn. Its velocity is around 40 nm/s and its motion is viscous (Fig. 2a-c). During its motion, an elastic distortion has been left at the sample surfaces giving rise to two straight and dark traces labeled $tr.P_2$. This indicates that the plane of motion of the dislocation is inclined with respect to the foil plane. From the variation of its apparent width and trace direction with specimen tilt, the plane of motion has been found to be the $(0, 1, 0, \bar{1}, 0, 0)$ two-fold plane P_2 , of direction $[1/1, 0/\bar{1}, 1/0]$ (see stereographic projection on Fig. 2j). During its motion, the dislocation remains straight along the 2-fold direction labeled u . According to the invisibility criterion $\vec{G} \cdot \vec{B} = 0$, the two strong extinctions in \vec{g}_{2a} and \vec{g}_{5a} (Fig. 2d and e) lead to a Burgers vector $\vec{b}_{\parallel 1}$ perpendicular to \vec{g}_{2a} and \vec{g}_{5a} , *i.e.* parallel to the direction $[1/1, 0/\bar{1}, 1/0]$ (Fig. 2j). This Burgers vector is perpendicular to the plane of motion. This proves that the dislocation has moved by climb. Single contrast conditions ($\vec{G} \cdot \vec{B} = 1$) in \vec{g}_{2b} and \vec{g}_{5a} (Fig. 2f and g) and double contrast conditions ($\vec{G} \cdot \vec{B} = 2$) in $\tau\vec{g}_{2c}$ and $\tau\vec{g}_{2d}$ (Fig. 2h and i) finally lead to $\vec{B}_1 = (0, 1, 0, \bar{1}, \bar{1}, \bar{1})$. Its component in the physical space is $\vec{b}_{\parallel 1} = [1/0, 1/\bar{1}, 2/\bar{1}]$ of length 0.297 nm. The same dislocation has already been found in samples deformed at lower temperature (see [24]). From this and other experiments [25, 26], the following conclusions can be drawn:

- Dislocations move by climb in 2-, 3- and 5-fold planes. Glide is at least 1000 times slower than climb in similar conditions.
- Dislocations are straight along dense directions (mostly 2-fold directions). This implies the existence of Peierls valleys along which dislocations are more stable. The rectilinear aspect of dislocations during their motion suggests, by analogy with dislocation motion in covalent and BCC crystals, that dislocation velocity is controlled by a difficult jog pair nucleation over the Peierls valleys followed by their easy diffusion along the line like in BCC structures.

3 Reconstructed electron density around dislocations

As perfect quasicrystal, we use a polyhedral model recently proposed by Quiquandon et al. [15] for i -AlPdMn. The model is a chemical decoration of a skeleton of interconnected atomic clusters of two kinds, B (Bergman) and M (Mackay) (see [16, 17]). The chosen decoration leads to a remarkably reduced number of local *chemical*

1
2
3
4
5
6
7
8 configurations: a single major chemical configuration for each of the
9 $M(M')$ -type clusters and only four for the B -type cluster. It fits
10 the experimental optimal composition $\text{Al}_{70.35}\text{Pd}_{21.36}\text{Mn}_{8.29}$ and has
11 reasonable reliability factors for both X-rays and neutrons diffraction
12 spectra. Details on the model are to be found elsewhere [15].

13 To visualize the atomic displacements and rearrangements around
14 a quasicrystalline dislocation, an image reconstruction is performed
15 by Fourier transforming the scattering structure factors $F(\vec{Q})$ of the
16 model multiplied by the phase factors due to the $6D$ -displacement
17 associated with the dislocation:
18
19

$$20 \quad \varrho(\vec{R}) = \left| \sum_k F(\vec{Q}_k) e^{2i\pi(\vec{Q}_k \cdot (\vec{R} + \vec{U}(\vec{r}_{\parallel})))} \right|^2$$

21 where \vec{Q}_k are the $6D$ -wavevectors of the reciprocal $6D$ -lattice and
22 $\vec{U}(\vec{r}_{\parallel})$ the total $6D$ displacement field. This procedure has been first
23 used by Devaud-Rzepski et al. [27] in the early 90's on simple quasi-
24 lattice models and developed in much details by Yang et al. [28] on
25 more realistic spherical atomic models. The interest of that kind of
26 calculations is that images can be computed in which the two fields
27 in E_{\parallel} and E_{\perp} can be separated thus allowing to separate visually the
28 phonon field from the phason field in E_{\parallel} . The present calculations do
29 not differ basically from the previous cited ones except that the struc-
30 tural atomic model is slightly more elaborated and the calculations
31 are made with a large number of Fourier terms of the electron density,
32 enough for localizing individual atoms.
33
34

35 The displacement phonon field in E_{\parallel} is approximated by that of
36 an ideal isotropic elastic medium. For straight dislocation lines, it is
37 independent of the location of the running point with respect to its
38 component along the line \vec{v}_{\parallel} and can thus be expressed as a function
39 of the two cylindrical variables defined in the plane perpendicular to
40 the dislocation line and passing through the running point. With the
41 notations of Fig. 3 we use the standard formula:
42
43

$$44 \quad 2\pi\vec{u}_{\parallel}(\rho, \theta) = \vec{b}_{\parallel}\theta + \frac{\vec{b}_{\parallel,e} \sin 2\theta + (\vec{b}_{\parallel} \wedge \vec{v}_{\parallel})(2(1-2\nu) \log \rho + \cos 2\theta)}{4(1-\nu)}$$

45 where $\vec{b}_{\parallel,e}$ is the edge part of \vec{b}_{\parallel} :
46
47

$$48 \quad \vec{b}_{\parallel,e} = \vec{b}_{\parallel} - (\vec{b}_{\parallel} \cdot \vec{v}_{\parallel})\vec{v}_{\parallel},$$

49 and $\rho = \sqrt{x^2 + y^2}$ and $\theta = \arctan y/x$ with:
50
51

$$52 \quad x = \vec{r}_{\parallel} \cdot \vec{b}_{\parallel,e} / |\vec{b}_{\parallel,e}|, \quad y = \vec{r}_{\parallel} \cdot (\vec{b}_{\parallel} \wedge \vec{v}_{\parallel}) / |\vec{b}_{\parallel} \wedge \vec{v}_{\parallel}|.$$

For the phason displacement field (in E_{\perp}), we use here the simplest pure screw model²:

$$2\pi\vec{u}_{\perp}(\vec{r}_{\parallel}) = \vec{b}_{\perp}\theta$$

The effect of each of the displacement fields in E_{\parallel} and E_{\perp} are exemplified on Fig. 4. The Fourier reconstruction of Fig. 4a has been computed in including only the phase shift of the parallel space contribution \vec{b}_{\parallel} (phonon field). A strong misfit of the atomic clusters is observed at the level of the Volterra (arbitrary) cut surface shown as a light gray line, that generates a phason wall along the line. This phason wall is very similar to a classical stacking fault boundary with the exception that the components of the fault vector have the form $(n + m\tau)/d$ where n , m and d are integers. Close to the dislocation core located at the center of the image, there exist a significant local deformation of the cluster shapes due to the elastic field of the dislocation. This, of course, is physically irrelevant since in that core region, linear elasticity is no longer valid.

The Fourier reconstruction of Fig. 4b uses the same model but has been computed with the perpendicular component \vec{b}_{\perp} only, the phason field. One observes again a strong misfit at the level of the Volterra cut that shows, like in the previous case and as expected, that the closure of the 6D hyper-crystal is not achieved by the sole \vec{b}_{\perp} component. As this displacement field extends only in E_{\perp} and in contrast to the previous case, there are no changes in the shape of the atomic clusters that are everywhere identical to those of the perfect quasicrystal. The difference here is in the way they are connected together.

The image of a perfect dislocation is fully recovered on picture (c) when both components \vec{b}_{\parallel} and \vec{b}_{\perp} are taken into account. In that case, the trace of the Volterra cut surface disappears because of the proper restacking issued from the perpendicular translation and the deformation spread out all over the atomic clusters as expected by the generated elastic field.

Figure 5 shows a high resolution reconstructed image of the electron density of the *i*-AlPdMn projected along the 3 basic high symmetry directions around a typical other dislocations of Burgers vector $\vec{B} = (0, 0, 1, 0, 0, \bar{1})$ of parallel component $\vec{b}_{\parallel} = [0/0, 2/0, 0/0]$ with $|b_{\parallel}| = 0.4795$ nm and $|b_{\perp}| = 0.7759$ nm.

The dislocation seen on Fig. 6 are partial dislocations of Burgers vectors $\vec{B}_1 = (\bar{1}, 1, 1, 1, 1, \bar{1})/2$ and $\vec{B}_2 = (1, 0, 0, 0, 0, 0)$; they are the

²There are *a priori* no basic physical reasons for choosing this particular law except that it can be reasonably assumed that the phason field spreads out isotropically around the dislocation line.

1
2
3
4
5
6
7
8
9
10
11
12
13
14
15
16
17
18
19
20
21
22
23
24
25
26
27
28
29
30
31
32
33
34
35
36
37
38
39
40
41
42
43
44
45
46
47
48
49
50
51
52
53
54
55
56
57
58
59
60

termination of fault planes with the same fault vectors drawn in light grey on the picture. These two faults correspond to the well-known planar defects with π fringes as antiphase boundaries in ordinary crystals.

4 Conclusion

Dislocations are defined in quasicrystals in much the same way as they are in ordinary crystals. Because of the additional dimensions needed to recover periodicity, the Burgers vector \vec{B} of a perfect dislocation is a translation of the high dimensional lattice, and decomposes into two irreducible components, \vec{b}_{\parallel} and \vec{b}_{\perp} , corresponding respectively to the phonon field in E_{\parallel} (standard elastic deformation) and the phason field developing in E_{\perp} (configurational thermodynamical energy). These two components are the physical bases of the dislocation motion mechanism that can be described as difficult jog pair nucleation over quasiperiodic Peierls valleys followed by a relatively easy diffusion along the line at high temperatures.

The geometrical framework of quasicrystalline dislocation description in high dimension spaces is presently well established. The understanding of the underlying physics governing their interactions and their modes of motion is at its beginning. This research field should open new original ways for studying the high temperature plastic behaviour of complex intermetallic phases with large unit cells which share many geometrical properties with quasicrystals.

References

- [1] D. Shechtman, I. Blech, D. Gratias, and J. W. Cahn. *Phys. Rev. Lett.*, **53**:1951–1954 (1984).
- [2] D. Shechtman and I. Blech. *Met. Trans.*, **16A**:1005–1012 (1985).
- [3] M. Wollgarten, Z. Zhang and K. Urban, *Phil Mag Lett*, **65**(1) 1–6 (1992).
- [4] M. Wollgarten, M. Beyss, K. Urban, H. Liebertz and U. Kocster, *Phys. Rev. Lett.*, **71**, 543 (1993).
- [5] T. C. Lubensky, S. Ramaswamy, and J. Toner. *Phys. Rev. B*, **33**:7715–7719 (1986).
- [6] J. E. S. Socolar, T. C. Lubensky, and P. J. Steinhardt. *Phys. Rev. B*, **34**:3345–3360 (1986).

- 1
2
3
4
5
6
7
8
9 [7] M. Kléman, M. in Proceedings of the ILL/Codest Conference
10 (Grenoble) Edited by C. Janot and J. M. Dubois, World Scien-
11 tific(Singapor), 318-326 (1988).
- 12 [8] M. Kleman and K. Sommers *Acta Met. Mat.* **39**, 287 (1991).
- 13 [9] M. Duneau and A. Katz, *Phys. Rev. Lett.* **54**, 2688-2691 (1985);
14 A. Katz and M. Duneau, *J. Phys. France* **47**, 181-196 (1986).
- 15 [10] P. A. Kalugin, A. Y. Kitayev and L. S. Levitov, *JETP Lett.* **41**,
16 145 (1985); *ibid. J. Phys. Lett. France* **46**, L601 (1985).
- 17 [11] V. Elser, *Acta Cryst. A* **42**, 36 (1986).
- 18 [12] P. Bak, *Phys. Rev. B* **32**, 5764 (1985); *ibid. Scripta Met.* **20**,
19 1199-1204 (1986); *ibid. Physica B&C* **136**, 296-300 (1986).
- 20 [13] J. E. S. Socolar, P. J. Steinhardt and D. Levine, *Phys. Rev. B* **32**
21 5547 (1985)
- 22 [14] J. W. Cahn, D. Shechtman and D. Gratias, *J. Mater. Res*, **1**, 13
23 (1986) .
- 24 [15] M. Quiquandon, J.-T. Beauchesne and D. Gratias, *Prototypical*
25 *simple atomic structure of i-AlPdMn*, in preparation.
- 26 [16] A. Katz and D. Gratias, *J. Non-Crystalline Solids* **153–154**, 187–
27 195 (1993).
- 28 [17] D. Gratias, F. Puyraimond, M. Quiquandon and A. Katz, *Phys.*
29 *Rev. B* **63** 024202-1–15 (2000).
- 30 [18] M. Feueurbacher, C. Metzmacher, M. Wollgarten, B. Baufeld, M.
31 Bartsch, U. Messerschmidt and K. Urban, K., *Mater. Sci. Engng*,
32 **A233**, 103 (1997).
- 33 [19] S. Takeuchi, R. Tamura and E. Kabutoya, *Phil. Mag.* **A82**, 379
34 (2002) ; see also S. Takeuchi, *Mater. Res. Soc. Symp. Proc.*, **553**,
35 283 (1999) .
- 36 [20] U. Koschella, PhD dissertation *Phason-elastische Energie in dek-*
37 *agonalen Quasikristallen*, Stuttgart University (2005).
- 38 [21] D. Caillard, G. Vanderschaeve, L. Bresson and D. Gratias, *Phil.*
39 *Mag.* **A80**, 237 (2000).
- 40 [22] D. Caillard, J. P. Morniroli, G. Vanderschaeve, L. Bresson and
41 D. Gratias, *Eur. Phys. J. Appl. Phys.*, **20**, 3 (2002).
- 42 [23] D. Caillard, C. Roucau, L. Bresson and D. Gratias, *Acta Mater.*,
43 **50**, 4499 (2002).
- 44 [24] F. Momprou, L. Bresson, P. Cordier and D. Caillard, *Phil. Mag.*,
45 **83**, 3133 (2003).
- 46
47
48
49
50
51
52
53
54
55
56
57
58
59
60

- 1
2
3
4
5
6
7
8 [25] F. Mompiou, M. Feuerbacher and D. Caillard, *Phil. Mag.*, **84**,
9 2777–2792 (2004) .
10
11 [26] F. Mompiou and D. Caillard, *Phil. Mag. Lett.*, **84**, 555 (2004).
12
13 [27] J. Devaud-Rzepisky, M. Cornier-Quiquandon and D. Gratias in
14 *Quasicrystals and incommensurate structures in condensed mat-*
15 *ter*, edited by M. J. Yakaman, D. Romen, V. Castano, A. Gomez,
16 (Singapore: World Scientific) p.498 (1990).
17
18 [28] W. Yang, M. Feuerbacher, N. Tamura, D. H. Ding, R. Wang and
19 K. Urban, *Phil. Mag. A*, **77**, 1481 (1998).
20
21
22
23
24
25
26
27
28
29
30
31
32
33
34
35
36
37
38
39
40
41
42
43
44
45
46
47
48
49
50
51
52
53
54
55
56
57
58
59
60

Figure 1: Example of an hypothetical dislocation of Burgers vector $B = (0, 0, 1, 0, 0, -1)$ (indexing scheme of [14]) seen end on in a 5-fold plane of an ideal atomic model of *i*-AlPdMn. This numerical reconstruction is computed using formula 3 including 141 beams of the 5-fold plane based on the structural model of *i*-AlPdMn. As in ordinary crystals, this "edge" dislocation is clearly visible at glancing angle as a discontinuity of atomic "planes".

Figure 2: Dislocation motion in the 2-fold plane P2 (a-c). Note the growth of the precipitate PR. The extinction condition (d-e), single (f-g) and double contrast conditions (h-i) lead to the burgers vector noted $b_{1\parallel}$ on the stereographic projection (j). The experimental determination of the Burgers vector together with the determination of the plane of motion of the dislocation shows that the motion process has a pure climb character.

Figure 3: Geometrical variables in E_{\parallel} used to calculate the displacement field of a dislocation of Burgers vector \vec{b} with a (straight) dislocation line along the unit vector \vec{v} . The local reference frame is defined by: z is along the dislocation line, x is the direction of the edge part of the dislocation, \vec{b}_e — and \vec{b}_s is its screw part — and y is the direction perpendicular to z and x . The running point \vec{r} is in the plane (x, y) and has cylindrical coordinates (ρ, θ) where the origin of the angle θ is taken along the positive x axis.

Figure 4: The various components of the phase shift induced by a perfect dislocation $\vec{B} = \vec{b}_{\parallel} + \vec{b}_{\perp} = (\bar{1}, 1, 0, 1, 1, 0)$ with $\vec{b}_{\parallel} = [\bar{2}/2, 0/2, 0/0]$ and $|b_{\parallel}| = 0.296381$ nm; $|b_{\perp}| = 1.25549$ nm of dislocation line $\vec{u}_{\parallel} = [0/0, 0/0, 1/0]$ in the *i*-AlPdMn model built with B-clusters (pentagons) and M-clusters (decagons). The dislocation is seen end-on in the 5-fold plane perpendicular to $(0, 1, \tau)$. Structural Fourier reconstruction: (a) phonon field: including only the \vec{b}_{\parallel} component, (b) phason field: including only the \vec{b}_{\perp} and (c) using both components. The light gray line is the trace of the Volterra cut surface: it appears as a line discontinuity on (a) and (b) reconstructions but, of course disappears in the full reconstruction (c).

Figure 5: High resolution calculated electron density of the *i*-AlPdMn model around a dislocation of Burgers vector $\vec{B} = (\bar{1}, 1, 0, 1, 1, 0)$ for from left to right the phonon (a,d,g), phasons (b,e,h) and total (c,f,i) displacement fields projected along the 5- fold (a,b,c), the 2-fold (d,e,f) and 3-fold (g,h,i) directions.

1
2
3
4
5
6
7
8
9
10
11
12
13
14
15
16
17
18
19
20
21
22
23
24
25
26
27
28
29
30
31
32
33
34
35
36
37
38
39
40
41
42
43
44
45
46
47
48
49
50
51
52
53
54
55
56
57
58
59
60

Figure 6: Reconstructed electron density of the *i*-AlPdMn model for partial dislocations of Burgers vectors $(\bar{1}, 1, 1, 1, 1, \bar{1})/2$ and $(1, 0, 0, 0, 0, 0)$ seen perpendicular to a 2-fold direction.